SUPPLEMENTAL MATERIAL

AcvR1-mediated BMP signaling in second heart field is required for arterial pole development: Implications for myocardial differentiation and regional identity

Penny S. Thomas, Sudha Rajderkar, Jamie Lane, Yuji Mishina, Vesa Kaartinen*

Department of Biologic and Materials Sciences, University of Michigan –Ann Arbor,

1011 N. University Ave, Ann Arbor, MI-48109, USA

*Corresponding author:

Vesa Kaartinen

Tel: 734-615-4726

Email: vesak@umich.edu

Supplemental Table 1 - Primary antibodies

	ID	Company	Dilution	retrieval	used here
α-smooth muscle α actin (mouse)	clone 1A4	Life tech	1:50	yes	cryo, wax
GFP (for YFP) (rabbit)	A11122	Life tech	1: 200	no	cryo
phospho-histone3 (rabbit)	#9701	Cell Signaling	1:50	(no)	cryo
phospho-histone3 (mouse)	#9706	Cell Signaling	1:50	(no)	cryo
Isl1 (mouse)	39.4D5	DSHB	1:200	yes (wax)	cryo, wax
phospho-Smad1/5/8 (rabbit)	#9511	Cell Signaling	1:100	yes (wax)	cryo
Sox9 (rabbit)	sc-20095	Santa Cruz	1:50	yes	cryo, wax
striated muscle myosin (mouse)	MF20	DSHB	1:200	(yes)	cryo, wax
WT1	sc-192	Santa Cruz	1:50	yes	cryo, wax

Supplemental Table 2 - In situ probes

	Length	Position	RefSeq	Source
Acvr1	600	815-1414	NM_001110204	
	851	1281-2124	NM_001110204	
Bmpr1a	618	407-1054	NM_009758	
	873	1122-1994	NM_009758	
Fgf8	785			Maruoka-Y et al (1998)
Fgf10	584	696-1264	NM_008002	(S Bellusci)
Isl1	600	301-899	NM_021459	
Nppa	600	first two exons		Zeller-R et al (1987)
Plexina2	>1000	<1524-4412	NM_008882	Addgene, Brown-CB et al 2001
Sema3c	875	322-1197	NM_013657	
Smad6	2190	739-2930	NM_008542	Thermofisher
Tdgf1	841	272-1113	NM_011562	
Tgfb2	730	1226-1955	NM_009367	
Wnt2	500			Tian et al (2010)
				Others cloned by the authors

Maruoka-Y et al (1998) Mech Dev 74, 175-7.
Zeller-R et al (1987) Genes & Dev 7, 693-8.
Tian-Y et al (2010) Dev Cell 18, 275-87.

Supplemental Table 3 – qRT-PCR primer sequences used

Gene	Forward	Reverse	Probe
Actb	tgacaggatgcagaaggaga	cgctcaggaggagcaatg	#106
Bambi	cgccactccagctacttctt	tgacgagcatcacagtagca	#71
Bmp2	cggactgcggtctcctaa	ggggaagcagcaacactaga	#49
Bmp4	gaggagtttccatcacgaaga	gctctgccgaggagatca	#89
Ccnd2	Mm00428070_ml Taqman assay		
Etv5	gcagtttgtcccagattttca	gcagctcccgtttgatctt	#10
Fgf8	tcctgcctaaactgacacaga	tgagctgatccgtcacca	#32
Fgf10	caagaaggaaaaacaggtgtgc	ttttcttctatgtttggatcgtca	#69
Hand1	gtgcgccctttaatcctctt	gtgcgccctttaatcctctt	#51
Isl1	agcaacccaacgacaaaact	ccatcatgtctctccggact	#83
Msx2	aggagcccggcagatact	gtttcctcaggtgcaggt	#70
Mycn	acctccggagaggatacctt	ccacatcgatttcctcctct	#69
Myh3	ggatgggaaagtcactgtgg	gtcctctggcttaaccacca	#18
Myh6	gggctggagcactgagag	gagagagaacaggcaggaa	#110
Myh7	cggatcaaggagctcacc	ctgcagccgcagtaggtt	#6
Myh11	tggaggccaacgattgcac	ggccgcctctttctctct	#25
Myl7	gggtggtgaacaaggaagag	gtgtcagcgcaaacagttg	#18
Nppa	cacagatctgatggatttcaaga	cctcatcttctaccggcatc	#25
Pea3	cagcaggaagccaccact	ggacttgatggcgatttgtc	#108
Smad6	gttgcaacccctaccacttc	ggaggagacagccgagaata	#70
Spry2	gagaggggttggtgcaaag	ctccatcaggtcttggcagt	#3
Srf	cagtggggaaaccaagga	gtagaggtgctgggtgctg	
Tbx1	gctctcccacgagttcaatc	acgtggggaacattcgtct	#104
Tbx2	cacaggggaacagtggatg	tctgcatggacttcaggatg	#97
	Mm000436915_ml Taqman probe		
Tbx3	ttgcaaagggttttcgagac	gactgcagtgtgagctgctt	#51
	Mm01195726_ml Taqman probe		
Tbx20	ccgtttgccaaaggattc	cactcactgttcaaatgagtaacctaa	#25
	ctatggggaagaggatgttctg	tcagatgttgtaaggctgatcc	#91
Tdgf1	ttttacgagccgtcgaagat	aattcaaacgcactggaatg	#47
Tgfb2	Mm00436955_ml Taqman probe		
Titin	agaagaaatttcctgtcatcaaaaa	tcttctctggctcaggttcttt	#110
Wnt2	cctgatgaaccttcacaacaac	tcttctttcagaagcgctttac	#11
Wnt2b	ccgggaccacactgtcttt	gctcagcacatagcatagacga	#16
Bmpr1a-cds	Mm00477650_ml Taqman assay		
5'-Bmpr1a	agctgttcggagaaattgga	cagaacaaaatcacttggcaat	#62
KI-Flag	ggacgacgatgacaagtgag	caacagatggctggcaacta	#98
KI-gen	tctgagtaggtgtcattctattctgg	tgctattgtcttcccaatcctc	#56
5'-Acvr1	tgcagtggatgagcagagag	actgctccaagggagaggag	#40
Acvr1-cds	attgaagggctcatcaccac	aagaccggagccacttcc	#94

(this assay does not involve the floxed allele in Acvr1^{Fl})

Online Figures

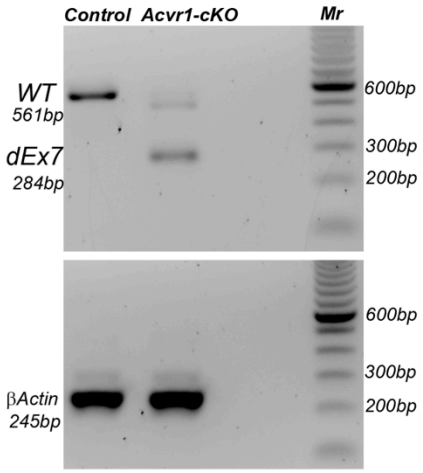

Online Figure 1. **The *Acvr1* conditional allele is efficiently recombined by *Mef2c[AHF]-Cre* in the OFT.** RT-PCR analysis of mRNA isolated from OFT at E10 in control (*Cre* negative) and mutant (*Acvr1-cKO)* embryos. Major amplification product of 284-bp produced the '*floxed'* exon 7 was detected in mutant embryos confirming an efficient *Mef2c[AHF]-Cre*-induced recombination (upper panel). Wild-type (WT) allele generated an expected 561-bp amplification product. βActin (amplification product of 245-bp) was used as a loading and quality control (lower panel).

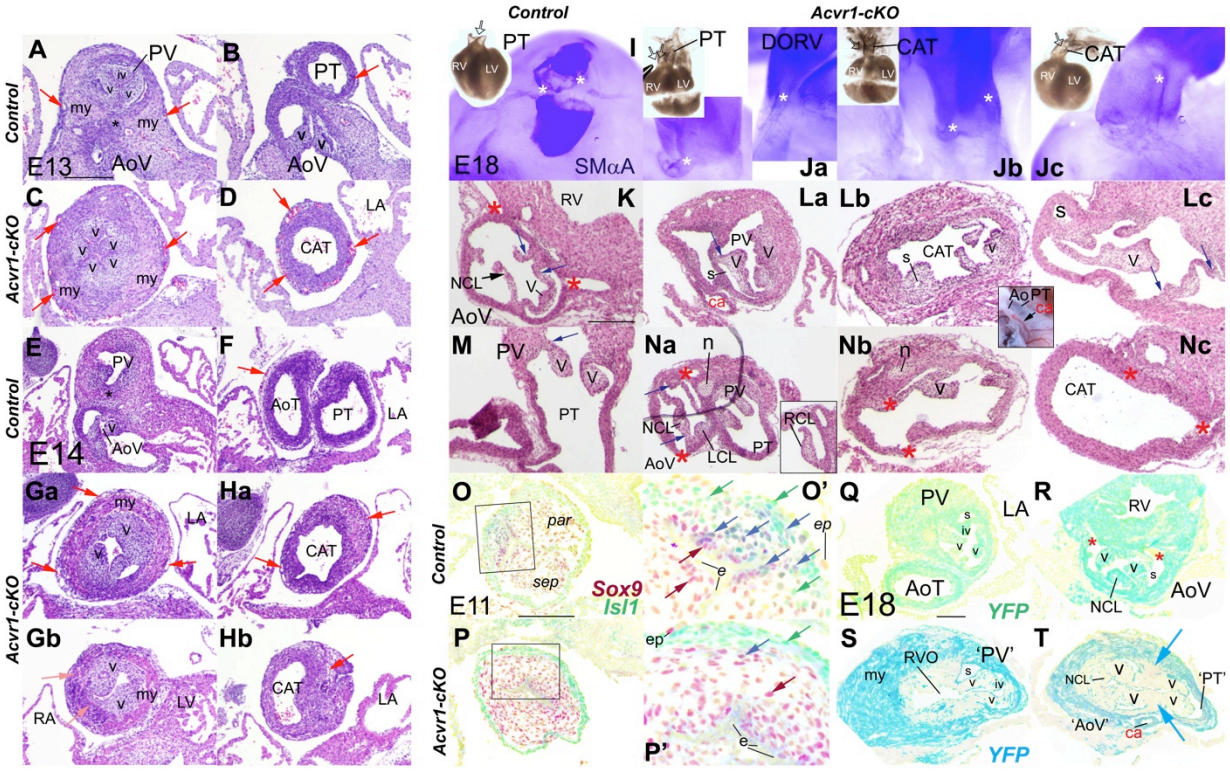

Online Figure 2. Variably abnormal valve, trunk and coronary development in *Acvr1-cKO.*
A-Hb, E13 and E14 sections transverse to OFT, H&E stain. In control (A,B; E,F) valves and trunks were completely septated, with only a small area of non-myocardial connection between the two valve at E13 (purple stain, asterisk, A) and a complete myocardial sleeve by E14 (E, asterisk). Each valve consisted of three leaflet cushions (V in A) and valves and trunks were at an angle to one another. In mutants without septation at this level, all valve leaflet cushions surrounded a common lumen (C), though still in groups slightly angled to one another. They were surrounded by wall composed of both myocardial (pink, my, pink arrows) and smooth muscle cell populations, variably intermixed (C, Ga, Gb). Trunk profiles and lumens also varied greatly in mutants (D,Ha, Hb) with prominent small, often blood filled, capillary-like spaces (red arrows), and myocardium (Ha) or irregular mixed tissue(Hb) externally.
I-Nc, E18 I-Jc, partially dissected wholemount (brightfield) and immunofluoresence for SmαA, arrow indicates direction of view, white asterisks coronary ostia. K-Nc sections of same hearts transverse to aortic or common valves, H&E. Control (I) heart had two coronary arteries, their ostia adjacent to the right and left (V) coronary leaflets of the aortic valve (K, red asterisks show circumferential position even if in not in section). In 'mild' *Acvr1*-cKO (DORV) phenotype, coronary ostia in near-normal locations around the aorta (red asterisks), though as the left coronary leafet (LCL) was only a small cushion, one opens above the enlarged NCL-positioned leaflet (Na). In more severe (CAT) mutants, ostia were sometimes on 'aortic side' of the common trunk (Nb), even when the aortic trunk was very small (inset, Lb), but could also appear displaced (Jc) and very distal to valve level (Jc). Although many had formed sinuses (s), valve leaflet morphology in *Acvr1*-cKO was also highly variable, from close to normal (NCL, RCL in Na) to abnormally small (LCL in Na), long, irregular profile (V in La,Lc) and variable thickness adjacent to valve wall (blue arrows). Note abnormal nodule-like cells adjacent to valves in some mutants (n in Na,Nb).
***Acvr1*-cKO affected contribution to OFT/valve cushion mesenchyme by SHF-derived cells.**
O-P', E11 transverse to OFT, immunofluorescence. In control (O, O') close to the most proximal part of the future aortic trunk and future intercalated leaflet cushion, in the many cells (blue arrows in O', enlargement of boxed area) co-express Isl1, otherwise restricted to SHF wall (green arrows), and Sox 9, otherwise restricted to epicardium and cushion mesenchyme (red arrows). In mutant (P), Isl1 and Sox9 co-expressing cells are hard to find.

Q-T, E18 transverse to 'OFT', immunofluorescence for YFP. In control (*Acvr1-cHet Mef2c[AHF]-Cre*$^{+}$*, R26R-YFP*$^{+}$*:* Q,R), recombined cells expressing YFP detected in RV myocardium, aortic and pulmonary trunk smooth muscle, and also to mesenchyme in valve leaflets (v, iv, V,NCL), especially those furthest from the other valve (iv, NCL). In mutant (*Acvr1-cKO*, *R26R-YFP*$^{+}$*:* S, T) myocardium and trunk smooth muscle recombined, very few mesenchymal cells in OFT cushion-derived valve leaflets (V,v,iv,NCL). Note that although OFT septation has failed (blue arrows mark position where fusion should have occurred), leaflet cushions have formed, three for each of a 'pulmonary' (S: PV, v,v,iv) and 'aortic' (T: V,V,NCL) valve sides of the common valve in this mutant. Much endocardium is recombined but little evidence for EMT from recombined endocardium or other SHF-derived cells in mutant.
AoV, aortic valve; CAT, common arterial trunk; DORV, double outlet right ventricle; e, endocardium; ep, epicardium; iv, intercalated leaflet (pulmonary); LV, left ventricle; my, myocardium; n, nodule-like cells; NCL, non-coronary leaflet; par, parietal OFT cushion; PT, pulmonary trunk, PV pulmonary valve; sep, septal OFT cushion; V,v,iv, valve leaflet/cushion. Yellow (where present), DAPI. Scale bar, 200μm.

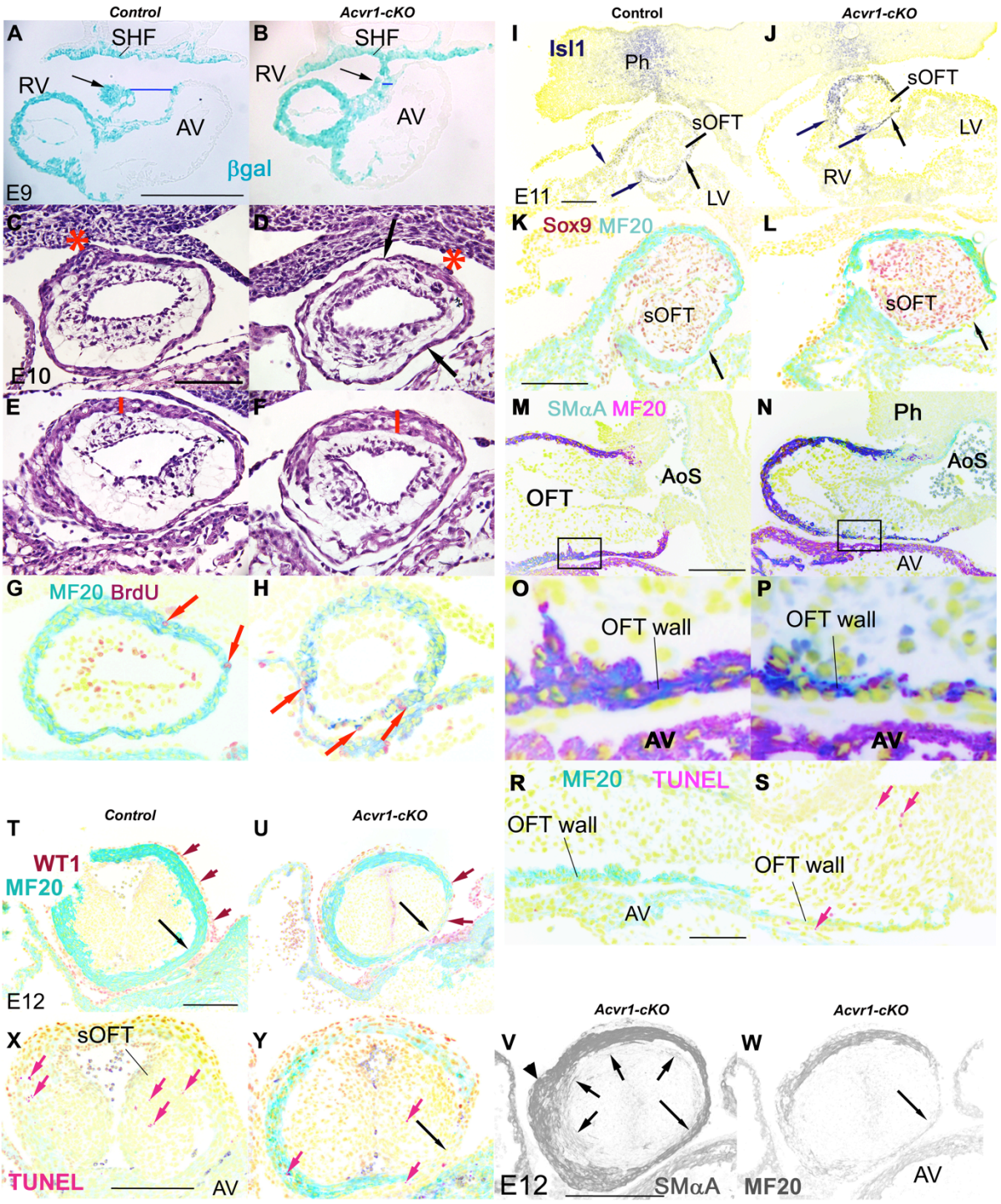

Online Figure 3. **Abnormalities in OFT wall in *Acvr1-cKO.***
A-B, E9, 4-chamber sections, βgal stain showing cells recombined by *Mef2c[AHF]-Cre*: Inner curvature in mutant (*Acvr1-cKO*, B) is narrower, as adjacent AV wall, RV and posterior OFT (arrow) are continuous, unlike control (*Acvr1-cHet* , A) where (AV) remains distant (blue lines). Note extent of recombination upstream of RV/OFT in general. C-H, E10 transverse to OFT; C-F H&E: distally (C,D), OFT wall thickness varies, from thick (*) to thin (one cell layer thick, arrow). More proximally, anterior wall is thicker (red bar)

in mutant (E vs. F). G-H: MF20 (blue), α-BrdU (pink) immuno-staining shows thin-walled, poorly differentiated region present only in mutant (H) contained proliferative cells (red arrows). I-S, E11; I-L transverse to OFT: Isl11 (blue) is expressed in very thin wall (black arrow) at mid OFT level in mutant (J) but MF20 very low (L) versus control (I). Isl1 expression higher in mutant OFT (J) than control (I), but subepicardial boundary (arrows) similar. Sox9 (red) expressed by cushion mesenchyme, some epicardium in both control (K) and mutant (L). M-S, sagittal to OFT, dorsal on the right: in mutant, thin myocardium along posterior mid-distal OFT expresses little SMαA (cyan) or MF20 (pink) (N, enlarged area P), control wall thicker with plentiful expression of both (blue) (M, enlarged area O). More TUNEL (pink arrows) staining in mutant (S) than control (R).
T-Y, E12, transverse to mid OFT: Thin wall in left/posterior position (black arrow) adjacent to septal cushion expresses much less MF20 (cyan) in mutant (U) relative to that in control (T), and poorly covered by WT1-positive (pink) epicardium (red arrows). Slightly more distal, right anterior wall irregularly thick (arrow head), relative expression of SMαA (grey) (V) and MF20 (grey) (W) varies with position around wall. Circumferentially oriented mesenchyme adjacent to wall also expresses SmαA (arrows). TUNEL labeling (pink arrows) present in both control (X) and mutant (Y) OFT mesenchyme and wall, but not higher in thin wall area.
AoS, aortic sac; AV, atrioventricular junction; RV, right ventricle; PhA, pharyngeal region; SHF, second heart field; SMαA, smooth muscle alpha actin; OFT, septal OFT cushion. Yellow (where present), DAPI. Scale bar 200μm, except C-H,R-S, 100μm.

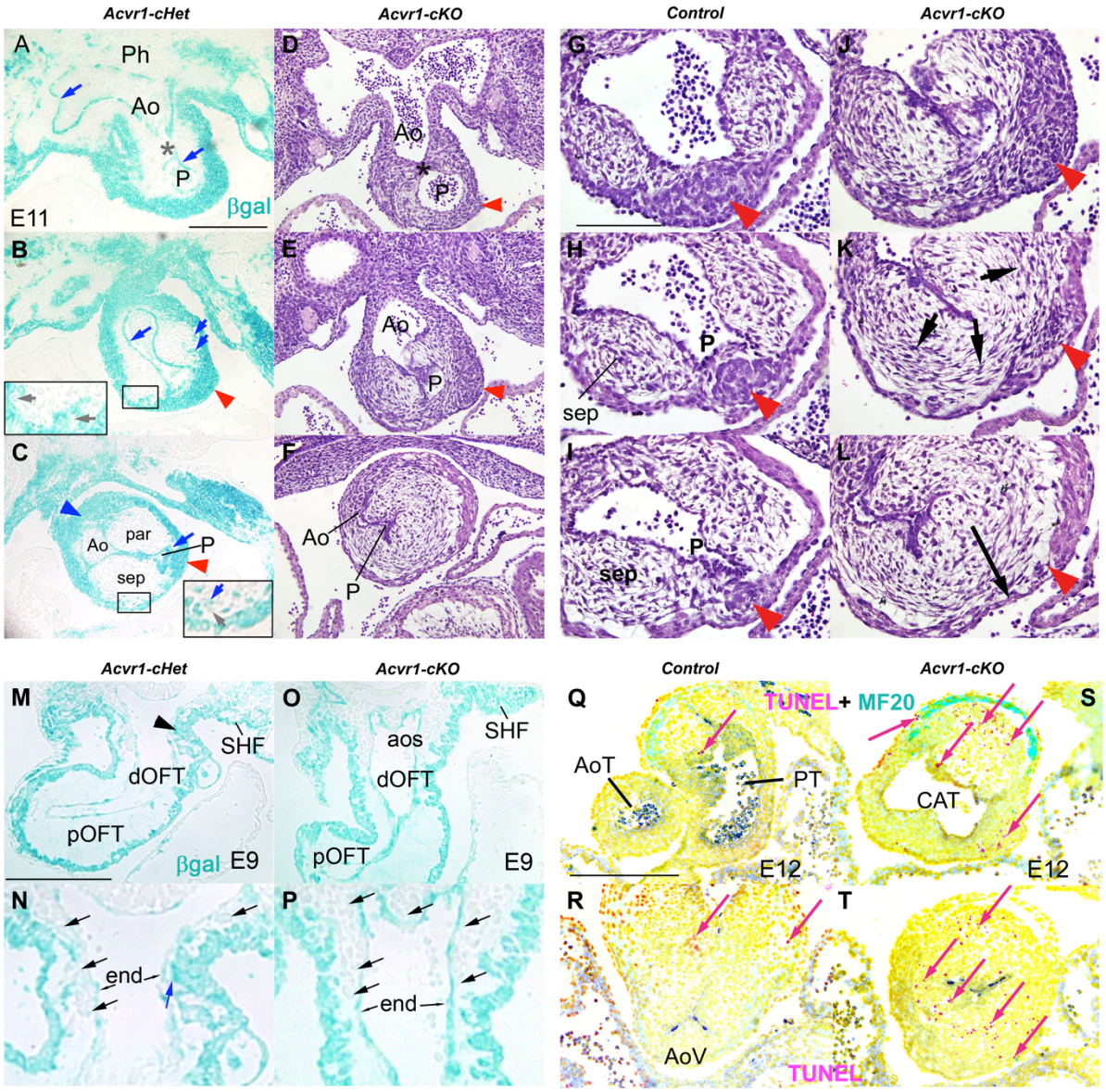

Online Figure 4. **Differences in cell populations at distal end of OFT between *Acvr1-cKOs* and controls.**
A-L, E11 sectioned transverse to OFT: A-C, *Acvr1-cHet Mef2c[AHF]-Cre* βgal stain, D-L, H&E: In control (A) distally, AP septation of the aortic sac level (*) formed separate aortic (Ao) and pulmonary (P) lumens. Recombined (blue) cells are SHF origin, including endothelium (blue arrows). More proximally (B,C), the AP septum was continuous with cushions that almost divided the OFT (par, sep) with the future trunk lumens lying close to thickened areas of recombined cells (blue and red arrow heads). Adjacent to these, recombined (small blue arrows) and unstained cells (grey arrows) lay locally intermixed (boxed area, detail shown enlarged). Note apparent anticlockwise twist in cushion position A-C. Distal AP septation (asterisk) had also commenced in mutant (D) but the distinctive population of cells adjacent to the pulmonary lumen (red arrowhead, E) was soon lost more proximally (by F), and the pulmonary lumen (P) displaced away from the wall by dysmorphic cushion. G-I, J-L: sections lie 56μm apart. In control sections (G-I), the endocardium remained close to a distinctive column of SHF cells (red arrow head; part of SHF population identified in A-E), as it narrows more proximally, ending immediately subjacent to myocardial

wall. In mutant (J-L), these column cells (red arrow head) appeared darker (J-K) and smaller (K) ending beneath a very thin layer of myocardium and over well-organized circumferentially aligned mesenchymal cells (L). Wall thickness was highly varied: compare thickness of myocardium anterior to the red arrow (L) with that posterior to it (black arrow). Compare this arrangement with the sagittal sections of the same region (Online Figure 3).

M-P, E9 parallel to OFT, *Mef2c[AHF]-Cre*-recombined bgal stain: In *Acvr1-cHet* control (M), SHF cells lay close to endocardium as they joined the OFT on embryo's left (arrowhead in M, blue arrow in N), which might affect neural crest cell migration, compare with embryo's right in higher mag view (N) black arrows mark unrecombined (neural crest) cells. In a mutant (O,P) of same somite stage, neural crest cells lay in between SHF and endocardium on both sides (black arrows) and adjacent to the pharyngeal endoderm.

Q-T, E12 transverse to OFT, TUNEL staining: Very little staining (pink arrows identify examples of distinctive pink spots of variable size) in control valve and trunk (Q), and mid-OFT valve-level tissues (R). In mutant, TUNEL staining plentiful in distal cushion, and irregularly thickened trunk wall in mutant (S) and in the mid-OFT cushions (T) including circumferentially oriented cell region, and adjacent left posterior wall below.

Ao, 'aortic' lumen; aos, aortic sac; AoT, aortic trunk; AoV, aortic valve; CAT, common arterial trunk; dOFT, distal, pOFT, proximal outflow tract; end, endocardium; P, 'pulmonary' lumen; par, parietal cushion; Ph, pharyngeal region; PT, pulmonary trunk; sep, septal cushion; SHF, second heart field. Yellow where present, DAPI. Scale bar 200μm, except G-L,N,P 100μm.

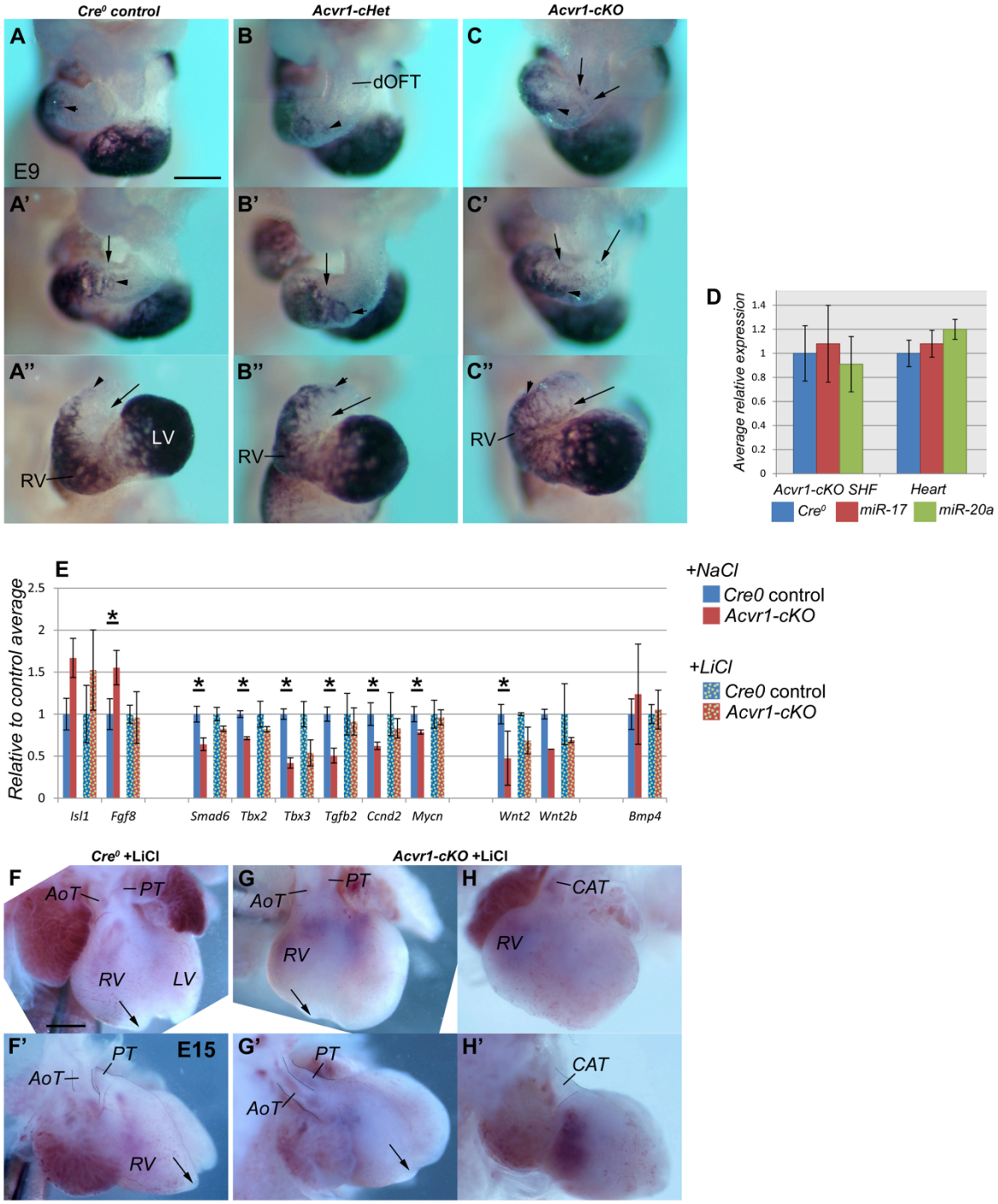

Online Figure 5. *Nppa* and *miR-17/20a* expression in, and the effect of LiCl-treatment on, controls and *Acvr1-cKOs.*

A-C", E9 WMT ISH for *Nppa,* A-C 4chamber, A'-C' oblique right, A'-C"oblique left/apical views. Ectopic expression of *Nppa* in mutant proximal-mid OFT. Arrowheads mark most distal extent of the narrow region of expression associated with proximal OFT in all genotypes. Arrows mark areas where positive expression present in mutant (C-C") but not in controls (*Cre*^{0}*, Acvr1-cHet:* A', A",B',B"). Note *Nppa* expression in RV in all genotypes.

D, Average *miR-17* (red bar), *miR-20a* (green bar) expression did not differ in E9 *Acvr1a-cKO* SHF-enriched, or heart tissues, relative to Cre0 equivalent control tissues (blue bar); n=3 each value,+-SEM.
E, qRT-PCR E9 RV+OFT. Maternal LiCl treatment partially normalized average expression of some genes at E9. NaCl-treated (control) samples: blue (control genotype), red (*Acvr1-cKO*); LiCl-treated samples: patched blue (control genotype), patched red (*Acvr1-cKO*). Average expression of *Fgf8*, *Tgfb2*, *Ccnd2*, *Mycn* in mutants differ in NaCl-treated but not LiCl-treated samples. LiCl-treated *Isl1* expression very variable. Average expression of other genes nearer to control values in LiCl-treated samples than NaCl-treated samples but still different (*Smad6*, *Tbx3*, *Wnt2*), * $p \leq 0.05$.
F-H, E15 4chamber and F'-H' from right: *Acvr1-cKO* heart septation and RV still abnormal following LiCl treatment, whether mild phenotype (DORV G,G') or severe (CAT, H,H'). Arrow marks position of RV apex (control F,F',G,G').
AoT, aortic trunk; CAT, common arterial trunk; dOFT distal OFT; LV, left ventricle; PT, pulmonary trunk; RV, right ventricle. Scale bar 200μm (A-C") or 500μm (F-H').

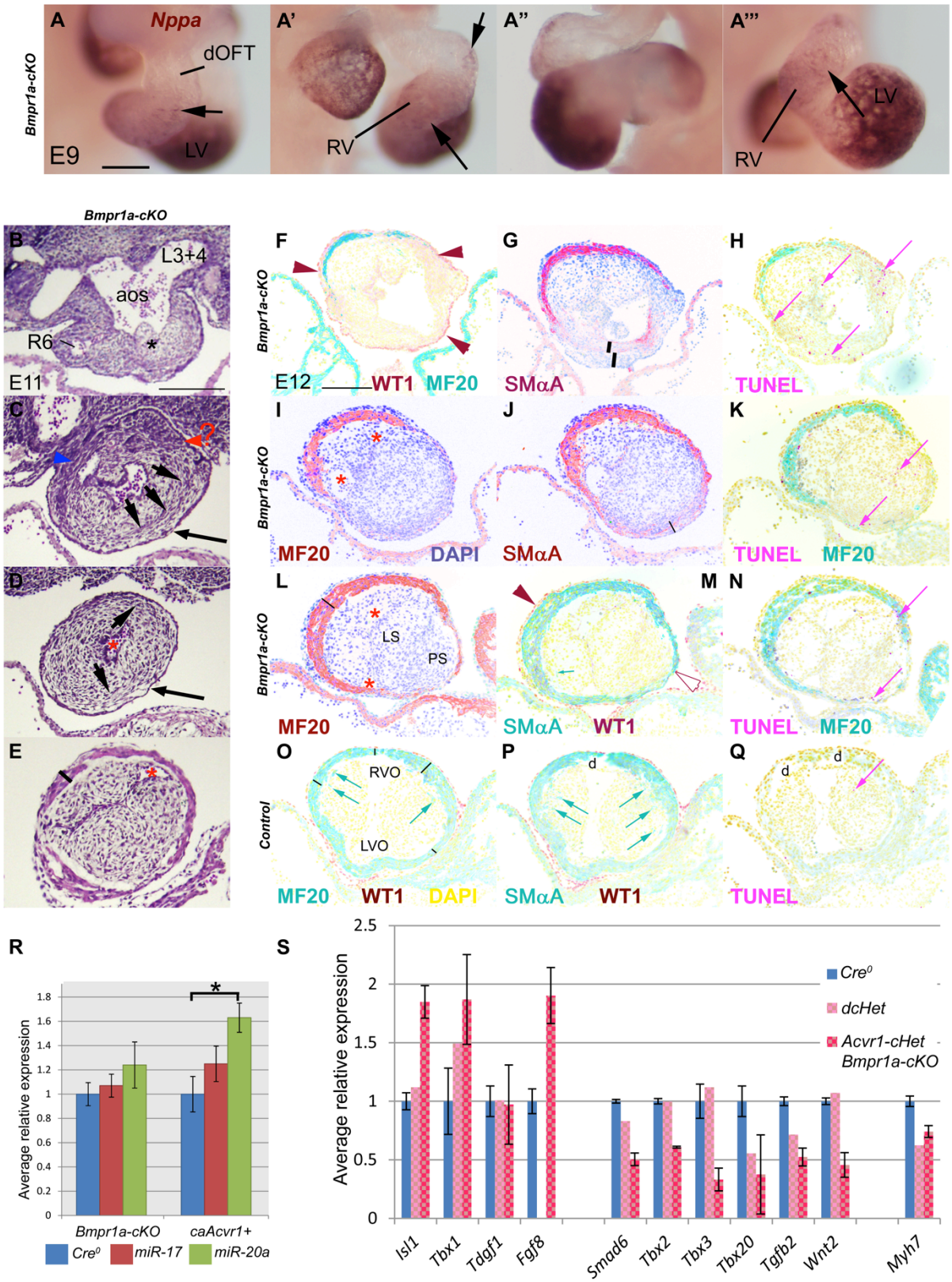

Online Figure 6. More extreme phenotype of *Bmpr1a-cKO.* A-A''', 4-chamber, right, left and apical views of E9 WMT ISH for *Nppa* in *Bmpr1a-cKO* showing very low *Nppa* expression in RV (long arrow)

and limited expression in proximal OFT (short arrow). Compare with control and *Acvr1-cKO* in online Figure 5, A-C.

B-E, E11 *Bmpr1a cKO* transverse to distal OFT, H&E: Distally, mesenchymal cells, likely neural crest-derived, occlude posterior of aortic sac (*), continuous with single cushion in distal OFT (C, D) which has displaced/unified lumens (red *), so connecting initially only with aortic part of aortic sac. In distal OFT, mesenchymal cells oriented circumferentially next to wall (short arrows, C,D). At mid-proximal OFT, separate cushions and variably positioned lumen(s) present, posterior/left cushion largest. OFT wall adjacent to aortic sac very thin anteriorly/right (C), composed of dark-staining cells, some in or near position of dense SHF cells identified in Online Figure 4 (blue, red arrowheads). Posterior and proximal to this (D) OFT wall very thin (long arrow) compared with controls (see Online Figure 4). At mid-proximal OFT junction level, where separate cushion present, wall multilayered and much thicker (E).

F-Q, E12 transverse to OFT, immunofluorescence: At level of valve/trunk junction (F-H), WT1-positive layer (red arrow heads, F) surrounded most myocardial, and all arterial wall of irregular thickness (black bars, G) some of which was SMαA-negative, and contained numerous TUNEL-positive areas (pink arrow, H) in mutant. More proximally (I-K), inconsistently composed wall (black bar, J) around very large posterior left OFT cushion expressed very little MF20 (K), and variable SMαA(L). Note TUNEL-positive areas (M). Mid-proximal OFT level (L-N) in mutant, largest OFT cushion consisted of two areas of mesenchyme, the luminal part (LS) resembling the smaller cushion, the parietal part (PS) with circumferentially oriented cells overlain by thin wall and very few WT1-positive cells (red arrowheads, M). Myocardial anterior-right wall very thick (bar, L). Some TUNEL staining in wall areas (pink arrows). In control sections at same level (N-P), wall thickness (black bars, N) varied much less (d,section damage) and was all MF20, SMαA-positive; some MF20, SMαA-positive cells extended into each cushion (blue arrows), unlike mutants, and very little TUNEL staining. See Online Figure 3 for other controls. DAPI shown blue (G,I,J,L) or yellow (F,H,K,M-Q). Empty space between wall and mesenchyme is artifactual.

R, Average *miR-17* (pink bar), *miR-20a* (green bar) expression did not differ in E9 *Bmpr1a-cKO* SHF-enriched samples relative to Cre^0 control tissues (blue bar); $caAcvr1^3$ SHF showed higher expression of *miR-20a*. n=3 each value,+/-SEM, * $P<0.05$.

S, qRT-PCR on E9 RV+OFT tissues samples lacking variable number of Bmp Type I receptor alleles. Results average of 3 (control), 2 (*Bmpr1a cKO,Acvr1-cHet*) and 1 (*Bmpr1a, Acvr1a dcHet*), error bars+/-SEM. Tissues containing only one *(Acvr1*) BMP Type I receptor allele show elevated or reduced expression similar to that of *Acvr1-cKO* and *Bmpr1a-cKO*, except average *Tdgf1* expression is not elevated, and *Myh7* is reduced.

aos, aortic sac; d, artifactual damage; dOFT, distal OFT; L3+4, left side common area of arch vessels 3 and 4; LS, luminal side of septal cushion; LVO, left ventricular outlet; PS, parietal side of septal cushion; RV, right ventricle; RVO, right ventricular outlet. Scale bar 200μm.

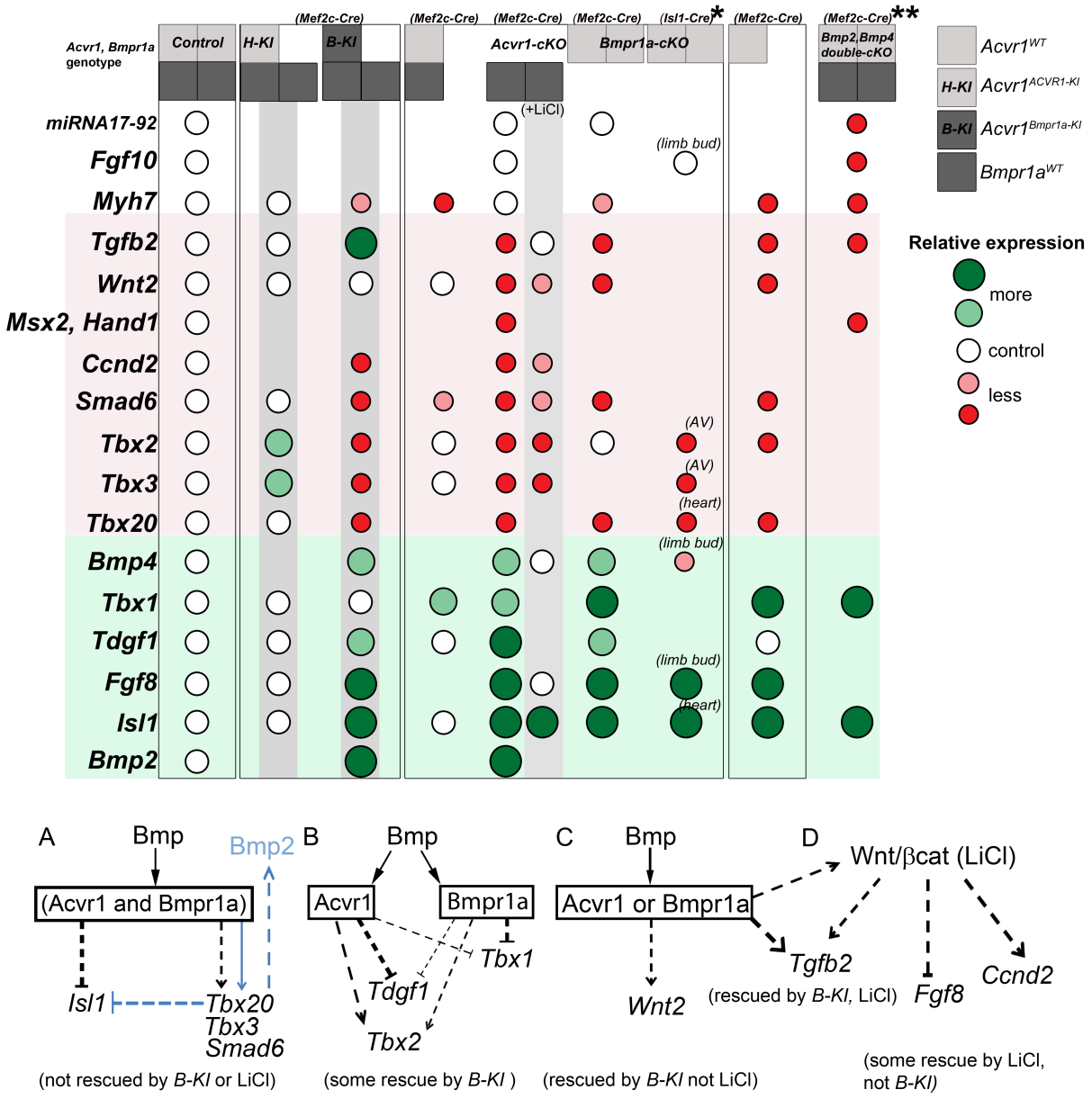

Online Figure 7. Sensitivity of gene expression to BMP signaling and possible regulatory networks.

Number of functional BMP Type I receptor alleles (*Acvr1*, pale grey square; *Bmpr1a*, dark gray square) decreases from left to right, following recombination by the driver (in brackets above the squares). Effect on gene expression in *cKO* relative to control (two functional *Acvr1*, two functional *Bmpr1a* alleles present) depicted using color/size: more by green, larger circles; less by pink, red smaller circles. Effect of 'rescue' on *cKO* expression shown with grey backgrounds: presence of *Acrv1-KI* ('H-KI'), *Bmpr1a-KI* ('B-KI') or following LiCl treatment ('+LiCl'). Data used are average qRT-PCR results from this paper, plus *WMT-ISH on limb bud, atrioventricular region and heart, and qRT-PCR from study by Yang et al (2006), and **qRT-PCR from Wang et al 2010 on *Bmp2*, *Bmp4*-double-cKO hearts. Most but not all showed increasingly severe effect as Bmp signaling is reduced (approximated by left to right axis); *Tdgf1* and *Tbx2* appeared more sensitive to loss of *Acvr1* than *Bmpr1a.*

Genes are grouped vertically according to effect of Acvr1-cKO (none, lower expression, higher expression) and then approximately in order of sensitivity to loss of BMP signaling, and ability to be

rescued. Expression of some genes (*miRNA17-92, Fgf10, Bmp4*) appeared relatively insensitive to reduction in BMP signaling; that of *Tgfb2* was reduced when only two alleles present but rescued by either LiCl or *Bmpr1a-KI*; *Tbx1* and *Wnt2* only rescued by LiCl treatment. Known direct BMP targets including *Tbx3* and *Tbx20* were not restored by the addition of *Bmpr1a-KI* or LiCl. These results also illustrate that *Fgf8* and *Isl1* appeared repressed by a non-*Tbx1*-dependent mechanism.

Cartoons A-D show 'regulatory relationships' implied by results from studies here (black lines). The mechanisms underlying the result may vary considerably, from direct regulation on gene expression to relative proportion of cells expressing the gene within the assayed population. Solid lines indicate direct regulation, dashed direct or indirect, blue lines implied by work of others.

A, Expression of one group of genes (*Isl1, Tbx20, Tbx3* and *Smad6*) appeared dependent on the presence of both *Acvr1* and *Bmpr1a*, as they were not were not restored to normal by the presence of *Bmpr1-KI* in *Acvr1-cKO*. Relevant results, from others are shown in blue. BMP signaling directly targets *Tbx20*, *Tbx2* [9, 10], and *Smad6*[11]. *Bmp2* expression can be dependent on Tbx2, Tbx3; Tbx20 repress *Tbx2* expression[9], and Tbx20 inhibit *Isl1* expression[12].

B, The relative average expression of other genes implies some Type I receptor specificity; *Tdgf1* and *Tbx2* appeared more sensitive to conditional loss of *Acvr1, Tbx1* to loss of *Bmpr1a*; rescue by either *ACVR1-KI* or *Bmpr1a-KI* also had different effects.

C, *Wnt2* levels were restored to control levels by *Bmpr1a-KI* but not LiCl treatment.

D, Three genes (*Tgfb2, Fgf8, Ccnd2*) may normally be regulated by BMP signaling via Wnt/βcat signaling as LiCl treatment normalized average expression, but only *Tgfb2* expression in *Acvr1-cKO* was also sensitive to *ACVR1-KI* and *Bmpr1a-KI*. That it became *over*-expressed in *Acvr1-cKO* only in the presence of *Bmpr1a-KI* may reflect an AcvR1-specific mechanism that also limits *Tgfb2* expression.

References for Supplemental Figure 7.

9. Singh R, Hoogaars WM, Barnett P, Grieskamp T, Rana MS, Buermans H, Farin HF, Petry M, Heallen T, Martin JF, Moorman AF, t Hoen PA, Kispert A, Christoffels VM. Tbx2 and tbx3 induce atrioventricular myocardial development and endocardial cushion formation. *Cell Mol Life Sci*. 2012;69:1377-1389
10. Yang L, Cai CL, Lin L, Qyang Y, Chung C, Monteiro RM, Mummery CL, Fishman GI, Cogen A, Evans S. Isl1cre reveals a common bmp pathway in heart and limb development. *Development*. 2006;133:1575-1585
11. Ishida W, Hamamoto T, Kusanagi K, Yagi K, Kawabata M, Takehara K, Sampath TK, Kato M, Miyazono K. Smad6 is a smad1/5-induced smad inhibitor. Characterization of bone morphogenetic protein-responsive element in the mouse smad6 promoter. *J Biol Chem*. 2000;275:6075-6079
12. Cai CL, Zhou W, Yang L, Bu L, Qyang Y, Zhang X, Li X, Rosenfeld MG, Chen J, Evans S. T-box genes coordinate regional rates of proliferation and regional specification during cardiogenesis. *Development*. 2005;132:2475-2487